Inorg. Chem. **2007**, *46*, 8569–8576

Room-Temperature Emission from Platinum(II) Complexes Intercalated into Zirconium Phosphate-Layered Materials

Eladio J. Rivera,[†] Cristina Figueroa,[†] Jorge L. Colón,*[,†] Levi Grove,[‡] and William B. Connick[‡]

Department of Chemistry, University of Puerto Rico, P.O. Box 23346, Río Piedras, Puerto Rico 00931, and Department of Chemistry, University of Cincinnati, P.O. Box 210172, Cincinnati, Ohio 45221-0172

Received March 31, 2007

The direct ion exchange of chloro(2,6-bis(*N*-methylbenzimidazol-2-yl)pyridine)platinum(II) ([Pt(Me$_2$bzimpy)Cl]$^+$) and chloro(2,2′:6′,2″-terpyridine)platinum(II) ([Pt(tpy)Cl]$^+$) complexes within a zirconium phosphate (ZrP) framework has been accomplished. The physical and spectroscopic properties of [Pt(Me$_2$bzimpy)Cl]$^+$ and [Pt(tpy)Cl]$^+$ intercalated in ZrP were investigated by X-ray powder diffraction and X-ray photoelectron, infrared, absorption, and luminescence spectroscopies. In contrast to unintercalated complexes in fluid solution, which do not emit at room temperature, both intercalated materials in the solid state and in colloidal suspensions exhibit intense emissions at room temperature. A [Pt(Me$_2$bzimpy)Cl]$^+$-exchanged ZrP colloidal methanol suspension gives rise to an emission at 612 nm that originates from a lowest ^{3}MMLCT[dσ^*(Pt) $\rightarrow$ π^*(tpy)] state (MMLCT = metal–metal-to-ligand charge transfer) characteristic of strong Pt···Pt interactions. A [Pt(tpy)Cl]$^+$-exchanged ZrP colloidal aqueous suspension exhibits a strong emission band at 600 nm. The accumulated data demonstrate that at high concentrations, [Pt(Me$_2$bzimpy)Cl]$^+$ and [Pt(tpy)Cl]$^+$ ions can serve as luminescent pillars inside the ZrP framework.

Introduction

Zirconium phosphate (ZrP)-layered materials are drawing increasing attention because of their ability to serve as ion exchangers, solid-state ion conductors, catalysts, photo- and biocatalysts, and hosts for the intercalation of a broad spectrum of guests.[1−3] To improve and expand upon this chemistry, there is strong motivation to develop new methods for tailoring the properties of the microheterogeneous environments of these materials. With this objective in mind, Colón et al. has recently demonstrated the first successful strategy for the direct ion exchange of inorganic complexes and organic molecules into zirconium bis(monohydrogen orthophosphate) monohydrate, $Zr(HPO_4)_2 \cdot H_2O$, also called α-zirconium phosphate (α-ZrP).[4−10] α-ZrP is composed of zirconium atoms in a semiplanar arrangement bridged by phosphate groups above and below the zirconium atom plane (Figure 1a). Each of the three oxygens of a phosphate group is bonded to a different zirconium, resulting in an octahedral coordination geometry around zirconium. The remaining oxygen atoms are directed into the interlamellar space just above or below the zirconium atoms in adjacent layers.[11] Figure 1b shows that a hydrated form of α-ZrP with six water molecules per formula unit (referred to as 10.3 Å-ZrP) has an interlayer distance of 10.3 Å.

To probe the microheterogeneous environments of these new intercalation materials, we have turned our attention to luminescent reporter molecules. Emissive square-planar platinum(II) pyridyl complexes, such as [Pt(tpy)Cl]$^+$ (tpy = 2,2′:6′,2″-terpyridine) and [Pt(Me$_2$bzimpy)Cl]$^+$ (bzimpy = chloro(2,6-bis(*N*-methylbenzimidazol-2-yl)pyridine) platinum(II) (Figure 2), are attractive in this capacity because of

* To whom correspondence should be addressed. E-mail: jlcolon@uprrp.edu.
[†] University of Puerto Rico.
[‡] University of Cincinnati.

(1) Alberti, G. *Acc. Chem. Res.* **1978**, *11*, 163−170.
(2) Clearfield, A. *Chem. Rev.* **1988**, *88*, 125−148.
(3) Clearfield, A. *Prog. Inorg. Chem.* **1998**, *47*, 371−510.
(4) Martí, A. A.; Colón, J. L. *Inorg. Chem.* **2003**, *42*, 2830−2832.
(5) Martí, A. Ph.D. thesis, University of Puerto Rico, Río Piedras, Puerto Rico, 2004.
(6) Bermúdez, R. A.; Colón, Y.; Tejada, G. A.; Colón, J. L. *Langmuir* **2005**, *21*, 890−895.
(7) Bermúdez, R. A.; Arce, R.; Colón, J. L. *J. Photochem. Photobiol., A:* **2005**, *175*, 201−206.
(8) Santiago, M.; Velez, M.; Borrero, S.; Díaz, A.; Casillas, C.; Hoffman, C.; Guadalupe, A.; Colón, J. L. *Electroanalysis* **2006**, *18*, 559−572.
(9) Martí, A.; Paralitici, G.; Maldonado, L.; Colón, J. L. *Inorg. Chim. Acta* **2007**, *360*, 1535−1542.
(10) Martí, A.; Rivera, N.; Soto, K.; Maldonado, L.; Colón, J. L. *Dalton Trans.* **2007**, 1713−1718.
(11) Troup, J. M.; Clearfield, A. *Inorg. Chem.* **1977**, *16*, 3311−3314.

10.1021/ic7006183 CCC: $37.00
Published on Web 09/19/2007

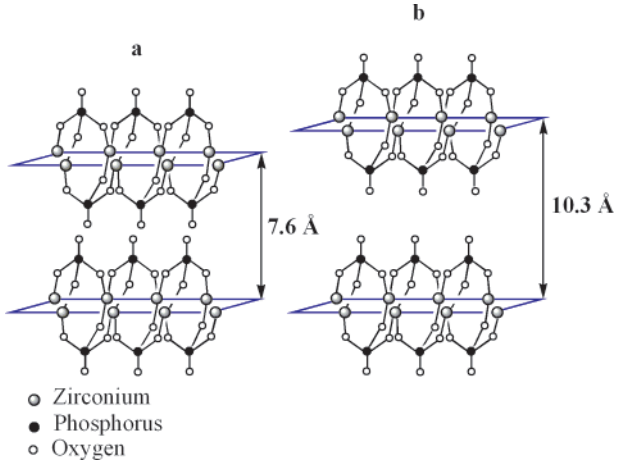

Figure 1. Idealized representation of two different ZrP phases: (a) α-ZrP and (b) expanded 10.3 Å-ZrP. Hydrogen atoms and water molecules are not shown for clarity.

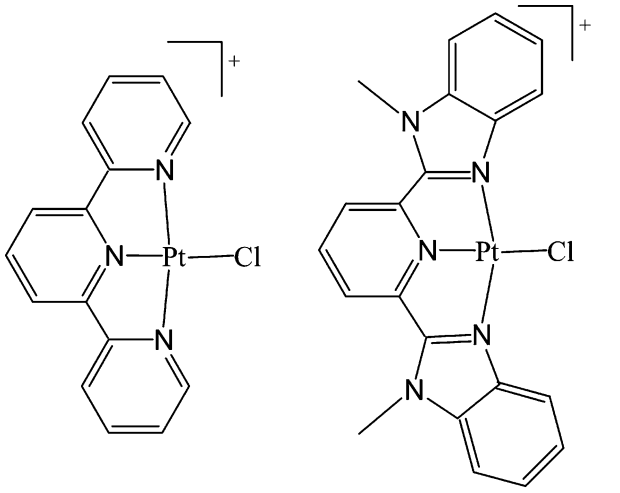

Figure 2. Drawings of platinum(II) complexes, $[Pt(tpy)Cl]^+$ and $[Pt(Me_2bzimpy)Cl]^+$.

the sensitivity of their spectroscopic properties to environment, as suggested by their interesting solution,[12−17] solid-state,[18−26] solid-support,[27−30] aggregation,[31−33] self-quenching,[34−36] and vapoluminescence[37−39] properties. The solution and solid-state photoluminescence from these compounds can originate from one of a variety of different lowest triplet excited states, including intraligand (IL), metal-to-ligand charge-transfer (MLCT), and metal−metal-to-ligand charge-transfer (MMLCT[dσ*(Pt) → π*(ligand)]) excited states.[18,19,24,34,38,40,41] A low-lying MMLCT excited-state can occur in dimers and aggregates with relatively short Pt···Pt separations (<3.5 Å). Interactions between the $5d_{z^2}$ orbitals of neighboring Pt(II) metal centers give rise to a dσ* highest-occupied molecular orbital, whereas the lowest-unoccupied molecular orbital is predominantly centered on the aromatic nitrogen-donor ligand. The resulting emission occurs at longer wavelengths than those of unimolecular ^{3}MLCT and ^{3}IL emissions.

In this paper, we report the direct ion exchange of $[Pt(tpy)Cl]^+$ and $[Pt(Me_2bzimpy)Cl]^+$ complexes into 10.3 Å-ZrP layers. At high loading levels, the complexes serve as pillars inside the ZrP framework. The resulting intense room-temperature luminescence is characteristic of strong intermolecular interactions, establishing the practical utility of this class of complexes as probes of the microenvironments of layered materials.

Experimental Section

Materials. Zirconium oxychloride octahydrate ($ZrOCl_2 \cdot 8H_2O$, 98%), 2,2′:6′,2″-terpyridine (tpy), and chloro(2,2′:6′,2″-terpyridine)-platinum(II) ($[Pt(tpy)Cl](Cl) \cdot 2H_2O$) were obtained from Aldrich Chemical Co. Phosphoric acid (H_3PO_4, 85% v/v) was obtained from Fisher. Chloro(2,6-bis(*N*-methylbenzimidazol-2-yl)pyridine)plati-

(12) Hill, G. M.; Bailey, J. A.; Miskowski, V. M.; Gray, H. B. *Inorg. Chem.* **1996**, *35*, 4585−4590.
(13) McMillin, D. R.; Moore, J. J. *Coord. Chem. Rev.* **2002**, *229*, 113−121.
(14) Michalec, J. F.; Bejune, S. A.; McMillin, D. R. *Inorg. Chem.* **2000**, *39*, 2708−2709.
(15) Hobert, S. E.; Carney, J. T.; Cummings, S. D. *Inorg. Chim. Acta* **2001**, *318*, 89−96.
(16) Yam, V. W.; Wong, K. M.; Zhu, N. *J. Am. Chem. Soc.* **2002**, *124*, 6506−6507.
(17) Yang, Q.; Wu, L.; Wu, Z.; Zhang, L.; Tung, C. *Inorg. Chem.* **2002**, *41*, 5653−5655.
(18) Houlding, V. H.; Miskowski, V. M. *Coord. Chem. Rev.* **1991**, *111*, 145−152.
(19) Miskowski, V. M.; Houlding, V. H. *Inorg. Chem.* **1989**, *28*, 1529−1533.
(20) Yip, H. K.; Cheng, L. K.; Cheung, K. K.; Che, C. M. *J. Chem. Soc., Dalton Trans.* **1993**, 2933−2938.
(21) Buchner, R.; Cunningham, C.; Field, J. S.; Haines, R. J.; McMillin, D. R.; Summerton, G. C. *J. Chem. Soc., Dalton Trans.* **1999**, 711−717.
(22) Lai, S. W.; Chan, M. C. W.; Cheung, K. K.; Che, C. M. *Inorg. Chem.* **1999**, *38*, 4262−4267.
(23) Field, J. S.; Haines, R. J.; McMillin, D. R.; Summerton, G. C. *J. Chem. Soc., Dalton Trans.* **2002**, *1369−1376*.
(24) Connick, W. B.; Marsh, R. E.; Schaefer, W. P.; Gray, H. B. *Inorg. Chem.* **1997**, *36*, 913−922.
(25) Field, J. S.; Gertenbach, J. A.; Haines, R. J.; Ledwaba, L. P.; Mashapa, N. T.; McMillin, D. R.; Munro, O. Q.; Summerton, G. C. *J. Chem. Soc., Dalton Trans.* **2003**, 1176−1180.
(26) Buchner, R.; Haines, R. J.; Ledwaba, L. P.; McGuire, R.; McMillin, D. R.; Munro, O. Q. *Inorg. Chim. Acta* **2007**, *360*, 1633−1638.
(27) Li, X.; Wu, L.; Zhang, L.; Tung, C.; Che, C. *Chem. Commun.* **2001**, 2280−2281.
(28) Zhang, D.; Wu, L.; Yang, Q.; Li, X.; Zhang, L.; Tung, C. *Org. Lett.* **2003**, *5*, 3221−3224.
(29) Che, C. M.; Fu, W.; Lai, S. W.; Hou, Y.; Liu, Y. L. *J. Chem. Soc., Chem. Commun.* **2003**, 118−119.
(30) Feng, K.; Zhang, R.; Wu, L.; Tu, B.; Peng, M.; Zhang, L.; Zhao, D.; Tung, C. *J. Am. Chem. Soc.* **2006**, *128*, 14685−14690.
(31) Wang, K.; Haga, M.; Monjushiro, H.; Akiba, M.; Sasaki, Y. *Inorg. Chem.* **2000**, *39*, 4022−4028.
(32) Bailey, J. A.; Hill, G. M.; Marsh, R. E.; Miskowski, V. M.; Schaefer, W. P.; Gray, H. B. *Inorg. Chem.* **1995**, *34*, 4591−4599.
(33) Arena, G.; Calogero, G.; Campagna, S.; Monsu, L.; Ricevuto, V.; Romeo, R. *Inorg. Chem.* **1998**, *37*, 2763−2769.
(34) Fleeman, W. F.; Connick, W. B. *Comments Inorg. Chem.* **2002**, *23*, 205−230.
(35) Chan, C. W.; Che, C. M.; Cheng, M. C.; Wang, Y. *Inorg. Chem.* **1992**, *31*, 4874−4878.
(36) Connick, W. B.; Geiger, D.; Eisenberg, R. *Inorg. Chem.* **1999**, *38*, 3264−3265.
(37) Kato, M.; Omura, A.; Toshikawa, A.; Kishi, S.; Sugimoto, Y. *Angew. Chem., Int. Ed.* **2002**, *41*, 3183−3185.
(38) Grove, L. J.; Rennekamp, J. M.; Jude, H.; Connick, W. B. *J. Am. Chem. Soc.* **2004**, *126*, 1594−1595.
(39) Wadas, T. J.; Wang, Q.; Kim, Y.; Flaschenreim, C.; Blanton, T. N.; Eisenberg, R. *J. Am. Chem. Soc.* **2004**, *126*, 16841−16849.
(40) Connick, W. B.; Henling, L. M.; Marsh, R. E.; Gray, H. B. *Inorg. Chem.* **1996**, *35*, 6261−6265.
(41) Field, J. S.; Haines, R. J.; Ledwaba, L. P.; McGuire, R., Jr.; Munro, O. Q.; Low, M. R.; McMillin, D. R. *Dalton Trans.* **2007**, 192−199.

num(II) ([Pt(Me$_2$bzimpy)Cl](Cl)·2.5H$_2$O) and 10.3 Å-ZrP were synthesized as previously reported.[4,38,42] All other reagents were of spectroscopic grade and were used without further purification.

Intercalation Procedure. ZrP was suspended in aqueous solutions of [Pt(tpy)Cl]Cl at various [Pt(tpy)Cl]$^+$/ZrP molar ratios (1:25, 1:10, 1:5, 1:1, and 5:1) with constant stirring at ambient temperature for 5 days producing [Pt(tpy)Cl]$^+$-intercalated ZrP materials with different loading levels. The same procedure was used to produce [Pt(Me$_2$bzimpy)Cl]$^+$-intercalated ZrP materials except that the ZrP was suspended in 1:1 ethanol/water solutions of [Pt(Me$_2$bzimpy)Cl]$^+$ at 1:30, 1:10, 1:5, and 1:1 [Pt(Me$_2$bzimpy)Cl]$^+$/ZrP molar ratios. The materials are referenced according to the molar Pt/ZrP concentration ratio of the mixture used in their preparation. For example, the 1:1 [Pt(tpy)Cl]$^+$-exchanged ZrP material was prepared by suspending 0.1 g of 10.3 Å-ZrP in 500 mL of a 5.1×10^{-4} M [Pt(tpy)Cl]$^+$ aqueous solution. The mixture was filtered, and the solid was washed with abundant nanopure water and dried at ambient temperature for 3 days.

Characterization. X-ray powder diffraction (XRPD) patterns were obtained using a Siemens D5000 powder diffractometer with Cu Kα radiation ($\lambda = 1.5406$ Å). All XRPD patterns were collected on a 2θ range of 2−45°. X-ray photoelectron spectroscopy (XPS) analysis was performed at the Materials Characterization Center of the University of Puerto Rico using the Physical Electronics PHI 5600 ESCA system equipment. Primary excitation was provided by a Mg anode (Kα radiation, 1253.6 eV) biased at 15 kV and at the power setting of 400 W. The spectra were collected in a fixed analyzer transmission mode on a hemispherical electroanalyzer. The carbon 1s signal at 285 eV was used as the internal reference.

The infrared spectra were obtained using a Bruker Tensor 27 infrared spectrometer coupled to a Helios Bruker FT-IR microscope. UV−vis spectrophotometric and steady-state luminescence measurements were performed on water suspensions (0.008%, w/v) of the intercalated material purged with N_2 (99.999%) for 15 min prior to the analysis. UV−vis absorption spectra were recorded using a Shimadzu UV-2401 PC spectrophotometer. Emission and excitation spectra of Pt(II) complexes-exchanged ZrP colloidal suspensions (0.008% w/v) at different loading levels were obtained using a SE-900 spectrofluorometer (Photon Technology International, PTI) with a 150 W xenon lamp as the excitation source and a PTI model 710 photon-counting detector with a Hamamatsu R1527P photomultiplier. For the solid-state samples, the intercalated material was placed at 45° from the excitation source and the detector, using a front-face illumination technique.

Results and Discussion

Synthesis. Samples of platinum(II) complex-exchanged ZrP were readily prepared from suspensions of ZrP in solutions of the chloride salts of [Pt(Me$_2$bzimpy)Cl]$^+$ and [Pt(tpy)Cl]$^+$. The loading level was controlled by varying the Pt/ZrP molar ratio used in the suspension over a wide range (1:30−5:1), and the materials are referenced according to this concentration ratio. The intercalation products were isolated by filtration to give red-orange microcrystalline samples of [Pt(Me$_2$bzimpy)Cl]$^+$ and orange microcrystalline samples in the case of [Pt(tpy)Cl]$^+$. To determine if [Pt(Me$_2$bzimpy)Cl]$^+$ or [Pt(tpy)Cl]$^+$ had undergone any chemical change during or after the intercalation process, FT-IR measurements of the intercalated materials were performed.

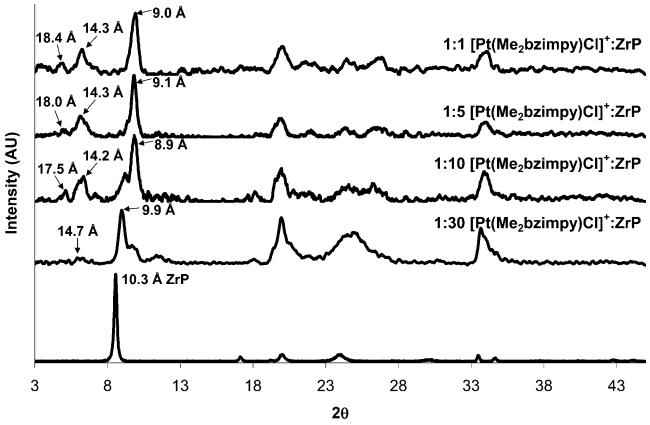

Figure 3. XRPD patterns of 1:30, 1:10, 1:5, and 1:1 [Pt(Me$_2$bzimpy)Cl]$^+$-exchanged ZrP and 10.3 Å-ZrP.[47]

As expected, the intensity of the bands associated with the platinum complexes increases with loading level (Supporting Information Figures S1 and S2, respectively), and no new bands are observed. Overall, the spectra are entirely consistent with the superposition of the spectra of the unintercalated ZrP and the respective platinum salts, with the exception that the "lattice" water band at 1617 cm^{-1} is significantly weaker at high loading levels. Combined with the XPS data, which show a 1:1 Pt/Cl molar ratio for all loading levels (vide infra), these results suggest that water is displaced during intercalation,[43] but neither [Pt(Me$_2$bzimpy)Cl]$^+$ nor [Pt(tpy)Cl]$^+$ is chemically modified.

X-ray Powder Diffraction. Figure 3 shows the XRPD patterns for 10.3 Å-ZrP and the [Pt(Me$_2$bzimpy)Cl]$^+$-exchanged ZrP samples from 1:30 to 1:1 Pt/ZrP molar ratios. The XRPD patterns show the formation of a mixed phase. At the lowest loading level (1:30 Pt/ZrP), the XRPD pattern shows an intense peak at an angle corresponding to a 9.9 Å interlayer distance with a shoulder at the high 2θ side corresponding to a distance of ca. 9.2 Å. In addition, it shows small peaks in the vicinity of the 14.7 Å region. The 9.9 Å peak is in agreement with the interlayer distance expected for ZrP intercalated with one ethanol molecule per formula unit previously observed by Costantino;[44] the [Pt(Me$_2$bzimpy)Cl]$^+$-exchanged ZrP samples were prepared in a 1:1 ethanol/water solvent. The 9.2 Å peak apparently is a second-order peak; the expected first-order peak at 18.4 Å is not seen at this low loading level but is observed at higher loading levels. As the loading increases, the peak at 9.9 Å, corresponding to the phase with intercalated ethanol, decreases while the peak at 9.2 Å increases, indicating that there are more layers with Pt(II) complex ions intercalated after displacing ethanol. In addition, the peaks in the 14.7 Å region become sharper, with the strongest peak varying from 14.2 to 14.3 Å. Since the intercalation process in ZrP is topotactic,[45] the increase in the interlayer distance from that of the wet unintercalated starting material (10.3 Å) indicates

(42) Kijima, T. *Bull. Chem. Soc. Jpn.* **1982**, *55*, 3031−3032.
(43) Horsley, S. E.; Nowell, D. V.; Stewart, D. T. *Spectrochim. Acta* **1974**, *30A*, 535−541.
(44) Costantino, U. *J. Chem. Soc., Dalton Trans.* **1979**, 402−405.
(45) Backov, R.; Bonnet, B.; Jones, D. J.; Roziere, J. *Chem. Mater.* **1997**, *9*, 1812−1818.

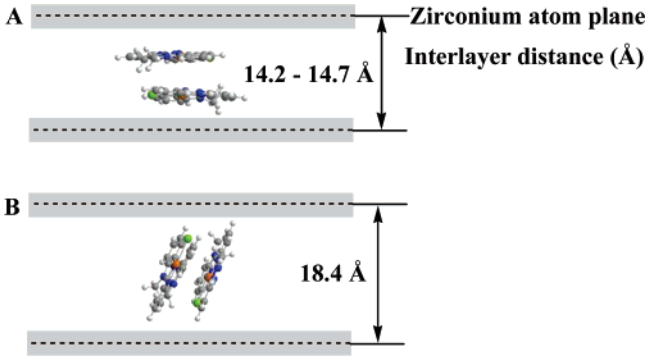

Figure 4. Idealized model of possible orientations of [Pt(Me$_2$bzimpy)Cl]$^+$ ions within the ZrP layers.

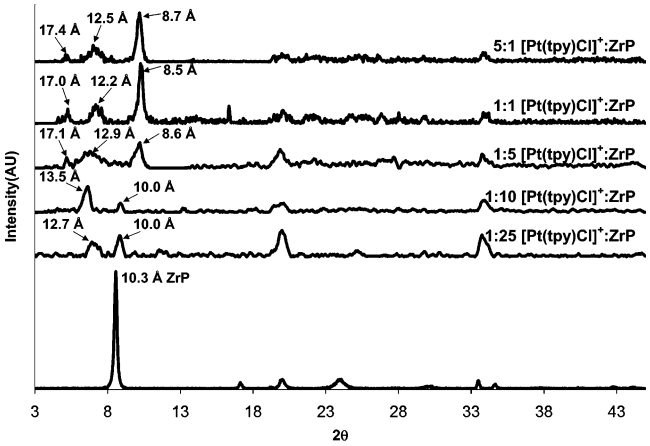

Figure 5. XRPD patterns of 1:25, 1:10, 1:5, 1:1, and 5:1 [Pt(tpy)Cl]$^+$-exchanged ZrP and 10.3 Å-ZrP.

that the [Pt(Me$_2$bzimpy)Cl]$^+$ complex is being intercalated between the layers of ZrP.

Is important to note that the interlayer distance is for the dry platinum-intercalated material. Unintercalated 10.3 Å-ZrP collapses into α-ZrP (with an interlayer distance of 7.6 Å) upon drying.[46] Since no 7.6 Å ZrP phase is observed in the XRPD patterns for the dry [Pt(Me$_2$bzimpy)Cl]$^+$-exchanged ZrP samples, these results indicate that the [Pt(Me$_2$bzimpy)Cl]$^+$ ions are intercalated and have expanded the interlayer distance of ZrP. The peaks at ca. 14.2 to 14.7 Å observed in Figure 3 are consistent with a phase in which the interlayer space is occupied by dimers of Pt complexes, with the two [Pt(Me$_2$bzimpy)Cl]$^+$ ions almost parallel to the ZrP layers and overlapping each other (Figure 4a). The thickness of a [Pt(Me$_2$bzimpy)Cl]$^+$ ion is estimated to be 4.2 Å.[47] Since the ZrP layer thickness is 6.6 Å,[48] having a dimer of ions parallel to the layers would give an interlayer distance of 15.0 Å (6.6 + 8.4 Å). The breadth and asymmetry of this feature is suggestive of slightly slipped stacked dimers with varying Pt···Pt distances. It should be noted that at the loading levels used, there is no evidence in the XRPD data for a phase with only the monomers of the [Pt(Me$_2$bzimpy)Cl]$^+$ complex within the ZrP layers.

The XRPD patterns for [Pt(Me$_2$bzimpy)Cl]$^+$-exchanged ZrP at the highest loading level show the formation of a new phase with an expanded interlayer distance of 18.4 Å (Figure 3). Since the ZrP layer thickness is 6.6 Å,[48] the [Pt(Me$_2$bzimpy)Cl]$^+$ ions are situated in the 11.8 Å interlayer space. The van der Waals dimensions of [Pt(Me$_2$bzimpy)Cl]$^+$ are 15.9 × 12.2 × 4.2 Å.[47] The 12.2 Å dimension is in agreement with the observed expansion in the interlayer distance.[49] Therefore, as the loading level increases, in order to accommodate more Pt complexes between the layers, it is proposed that the Pt complexes adopt an orientation with their Pt−Cl bond (along the 12.2 Å axis) nearly perpendicular to the ZrP layers (Figure 4b). Geometry arguments show that a 75.3° tilt angle of the 12.2 Å molecular axis with respect to the layers results in an interlayer distance of 18.4 Å, as observed experimentally. However, at this point, we cannot discard the possibility that the complexes adopt an orientation in which their coordination planes are close to parallel to the ZrP layers; in that case, a stack of three complexes between layers could account for the observed interlayer spacing.

Similar layer expansions were observed for the ion exchange of the [Pt(tpy)Cl]$^+$ metal complex into 10.3 Å-ZrP. Figure 5 shows the XRPD patterns for 10.3 Å-ZrP and [Pt(tpy)Cl]$^+$-exchanged ZrP samples from 1:25 to 1:10 Pt/ZrP molar ratios. The XRPD patterns show the formation of a mixed phase with interlayer distances greater than those of 10.3 Å-ZrP and α-ZrP, indicating that the [Pt(tpy)Cl]$^+$ ions have intercalated in ZrP. The patterns become sharper as the [Pt(tpy)Cl]$^+$/ZrP molar ratio increases. At low loading levels (from 1:25 to 1:10 Pt/ZrP), the XRPD patterns suggest the formation of a mixed phase with an expanded interlayer distance varying from 12.7 to 13.5 Å. This mixed phase also presents a peak corresponding to a 10.0 Å interlayer distance. The feature is most intense for the 1:25 Pt/ZrP molar ratio sample, and it gradually loses intensity with increasing loading, completing disappearing at a 1:5 Pt/ZrP molar ratio. Since the samples were prepared in aqueous solution, rather than an ethanol/water mixture, the peak is not attributable to an ethanol-intercalated phase. The dimensions of [Pt(tpy)Cl]$^+$ are roughly 13.8 × 11.1 × 3.4 Å.[32,47,50−54] Therefore, given the ZrP layer thickness (6.6 Å),[48] the phase at low loading levels, characterized by the 10.0 Å peak, is attributed to discrete planar [Pt(tpy)Cl]$^+$ ions lying parallel to the layers

(46) Clearfield, A.; Duax, W. L.; Medina, A. S.; Smith, G. D.; Thomas, J. R. *J. Phys. Chem.* **1969**, *73*, 3424−3430.
(47) As calculated using *SPARTAN'04* for Windows, version 01. 00. 03e, wavefunction, semi-empirical model with a PM 03 basis set.
(48) Yang, C.; Clearfield, A. *React. Polym., Ion Exch., Sorbents* **1987**, *5*, 13−21.
(49) For other intercalated materials ([Ru(bpy)$_3$]$^{2+}$, [28] PYMA,[29,30] [Ru(phend)$_2$bpy]$^{2+}$,[31] and MV^{2+} [32]), we previously observed that ionic, hydrogen bonding, and other electrostatic interactions between the cations and the layers can cause the distances between them to become somewhat smaller than those predicted from the van der Waals distances. In addition, nothing precludes the ligands from slightly interpenetrating the layers between the phosphate groups, further decreasing the interlayer distance. Similar effects may play a role in these platinum-exchanged ZrP materials.
(50) Cini, R.; Tzeng, B. C.; Fu, W.; Che, C. M.; Chao, H. Y.; Cheung, K. K.; Peng, S. M. *J. Chem. Soc., Dalton Trans.* **1999**, 1017−1023.
(51) Angle, C. S.; DiPasquale, A.; Rheingold, A. L.; Doerrer, L. H. *Acta Crystallogr., Sect. C* **2006**, *C62*, m340−m342.
(52) Cini, R.; Donati, A.; Giannettoni, R. *Inorg. Chim. Acta* **2001**, *315*, 73−80.
(53) Sengul, A. *Turk. J. Chem.* **2004**, *28*, 667−672.
(54) Wong, Y. S.; Lippard, S. J. *Chem. Commun.* **1977**, 824−825.

Table 1. Platinum/Phosphorus Molar Ratios Obtained from XPS for $[Pt(Me_2bzimpy)Cl]^+$-Exchanged ZrP and $[Pt(tpy)Cl]^+$-Exchanged ZrP Samples

$[Pt(Me_2bzimpy)Cl]^+-ZrP$		$[Pt(tpy)Cl]^+-ZrP$	
Pt/ZrP loading	Pt/P (XPS)	Pt/ZrP loading	Pt/P (XPS)
5:1		5:1	1:5
1:1	1:4	1:1	1:5
1:5	1:5	1:5	1:7
1:10	1:12	1:10	1:20
1:30	1:32	1:25	1:32

(Supporting Information Figure S3). The peaks at ca. 12.7−13.5 Å in Figure 5 at low loading levels are consistent with a phase in which the interlayer space is occupied by dimers of Pt complexes, with the coordination planes of the two stacked $[Pt(tpy)Cl]^+$ ions lying nearly parallel to the ZrP layers. As suggested for $[Pt(Me_2bzimpy)Cl]^+$, the observed variation in interlayer distance (12.7−13.5 Å) is attributed to slightly slipped stacked dimers with varying Pt···Pt distances, which is supported by molecular modeling. Summing the ZrP layer thickness (6.6 Å)[48] and the estimated height of the dimer (6.8 Å) gives an estimated interlayer distance of 13.4 Å, in agreement with our experimental results.

As the loading level is increased (from 1:5 to 5:1 Pt/ZrP) a new phase becomes evident with an interlayer distance 17.0−17.4 Å, with a sharp and intense second-order peak at 8.5−8.7 Å. The proportion of this phase with the ca. 17.0−17.4 Å interlayer distance increases in the mixed phase as the loading level is increased. The expanded interlayer distance (17.4 Å) of this new phase indicates that a different structure is adopted at high loading levels compared with that of low loading levels. Subtracting the thickness of a ZrP layer from the 17.4 Å interlayer distance obtained at high loading results in a remaining free interlayer distance of 10.8 Å.[49] Although the precise arrangement of the $[Pt(tpy)Cl]^+$ ions between the layers is not certain, the available interlayer distance can accommodate the 11.1 Å dimension of a $[Pt(tpy)Cl]^+$ ion,[32,47,50−54] which lies parallel to the Pt−Cl bond. Therefore, as the loading level increased, in order to accommodate more Pt complexes between the layers, it is proposed that the Pt complexes adopted an orientation with their Pt−Cl bond (the 11.1 Å axis) nearly perpendicular to the ZrP layers. Geometry arguments show that a 76.6° tilt angle of the 11.1 molecular axis with respect to the layers results in an interlayer distance of 17.4 Å, as observed experimentally. These results indicate that, at high concentrations, $[Pt(Me_2bzimpy)Cl]^+$ and $[Pt(tpy)Cl]^+$ ions can serve as pillars inside the ZrP framework.

X-ray Photoelectron Spectroscopy. Table 1 shows the Pt/P molar ratios of the $[Pt(Me_2bzimpy)Cl]^+$-exchanged ZrP materials as estimated from XPS measurements. The XPS data show that the Pt/P molar ratios for the 1:30, 1:10, 1:5, and 1:1 $[Pt(Me_2bzimpy)Cl]^+$/ZrP samples were 1:32, 1:12, 1:5, and 1:4, respectively, increasing monotonically with the Pt/ZrP concentration ratio of the mixture used in their preparation. The 1:1 $[Pt(Me_2bzimpy)Cl]^+$/ZrP sample shows a Pt/P molar ratio of 1.4, which indicates that for each $[Pt(Me_2bzimpy)Cl]^+$ complex there are 2.0 ZrP formula units, corresponding to replacement of 25% of the exchangeable protons.

The surface area occupied by one ZrP formula unit is 24 $Å^2$.[3] The area projected on the ZrP layers by a $[Pt(Me_2bzimpy)Cl]^+$ ion positioned with the Pt−Cl bond perpendicular to the ZrP layers is 15.9 × 4.2 $Å^2$ or 66.8 $Å^2$. This gives a theoretical maximum loading of 0.36 $[Pt(Me_2bzimpy)Cl]^+$ ions per formula unit. From the XPS data, the experimental loading is 0.49 $[Pt(Me_2bzimpy)Cl]^+$ ions per formula unit. Although the reason for this discrepancy is not certain, one possible explanation is that poor crystallinity of the intercalated material results in an increase in the surface area of the material and therefore the available ion-exchange sites. A decrease in crystallinity is consistent with a broadening in the first-order diffraction peaks in the XRPD patterns, with an increase in the loading level.[55]

Similar results were obtained from the XPS data for the $[Pt(tpy)Cl]^+$-exchanged ZrP samples (Table 1). The Pt/P molar ratios for the 1:25, 1:10, 1:5, and 1:1 $[Pt(tpy)Cl]^+$:ZrP samples were 1:32, 1:20, 1:7, and 1:5, respectively, increasing monotonically with the Pt/ZrP concentration ratio of the mixture used in their preparation. The Pt/P molar ratio plateaus at 1:5 for the 1:1 and 5:1 Pt/ZrP samples, suggesting that maximum loading occurs at one $[Pt(tpy)Cl]^+$ complex per 2.5 ZrP formula units, corresponding to replacement of 20% of the exchangeable protons.

The surface area occupied by one ZrP formula unit on the face of a layer is 24 $Å^2$.[3] The surface area projected on the ZrP layers by a $[Pt(tpy)Cl]^+$ ion positioned with the Pt−Cl bond perpendicular to the ZrP layers (90° angle with respect to the layers) is (13.8 × 3.4) $Å^2$ or 46.9 $Å^2$. This cross-sectional area gives a theoretical maximum loading of 0.51 $[Pt(tpy)Cl]^+$ ions per formula unit, which slightly exceeds the experimental value of 0.40, as determined by XPS measurements. This result suggests that maximum loading occurs at 80% capacity of the cations in this arrangement.

Absorption and Emission Spectroscopy. UV−vis absorption spectra of orange suspensions of the platinum complex-exchanged ZrP are characteristically broad with a tailing long-wavelength profile attributed to scattered light (Figure 6). Nevertheless, absorption features can be distinguished that are consistent with bands observed in the spectra of the respective platinum complexes in fluid solution. In the case of $[Pt(Me_2bzimpy)Cl]^+$-exchanged ZrP samples, the intensity of the absorption bands increases steadily over the range of investigated loading levels (from 1:30 to 1:1 Pt/ZrP). The IL charge-transfer bands (300−390 nm) and a low-energy MLCT band (450 nm) are in good agreement with the solution spectra,[38] and there is no discernible red shift. Interestingly, there is evidence of additional absorption near 550 nm that is not present in $10^{-5}-10^{-4}$ M $[Pt(Me_2bzimpy)Cl]^+$ methanol solutions. Low-energy transitions arising in this region have previously been attributed to low-lying

(55) Trobajo, C.; Khainakov, S. A.; Espina, A.; García, J. R. *Chem. Mater.* **2000**, *12*, 1787.

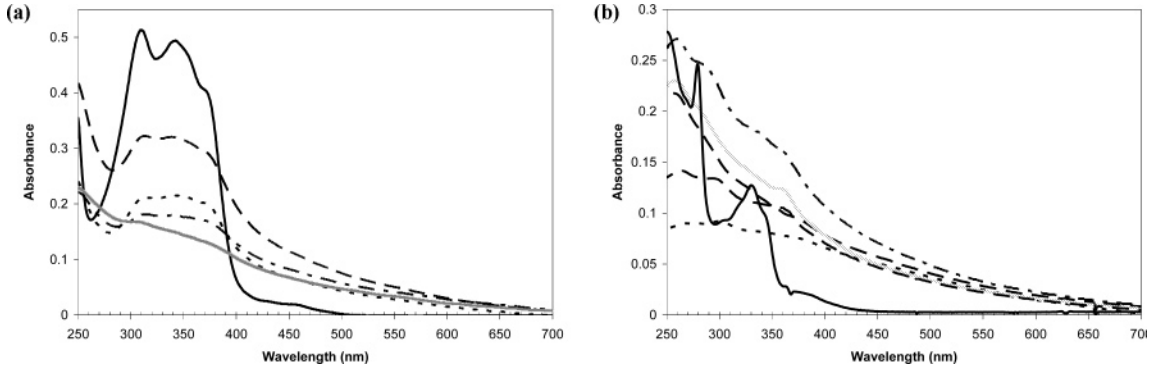

Figure 6. (a) UV−vis absorption spectra of $[Pt(Me_2bzimpy)Cl]^+$-exchanged ZrP methanol suspensions (0.008% w/v) at different loading levels: (— -, 1:1), (----, 1:5), (—, 1:10), and (••••, 1:30) and a 1.9×10^{-5} M $[Pt(Me_2bzimpy)Cl]^+$ methanol solution (—, solid line) at room temperature. (b) UV−vis absorption spectra of $[Pt(tpy)Cl]^+$-exchanged ZrP water suspensions (0.008% w/v) at different loading levels: (— —, 5:1), (----, 1:1), (— -, 1:5), (••••, 1:10), and (— —, 1:25) and a 1.9×10^{-5} M $[Pt(tpy)Cl]^+$ aqueous solution (—, solid line) at room temperature.

MMLCT transitions, resulting from dimers or oligomers with short Pt···Pt interactions.[38] These transitions are not resolved in the spectra of the suspensions due to the scattered light but are resolved in the spectra of the solid samples (vide infra).

In the case of the $[Pt(tpy)Cl]^+$-exchanged ZrP samples, at low loading levels (from 1:25 to 1:5 Pt/ZrP) the intensities of these features grows with increasing loading level. The manifold of tpy IL absorption bands in the 260−370 nm region[15] is red-shifted by ~1200 cm^{-1} from those of the aqueous solution spectrum of $[Pt(tpy)Cl]^+$. The red shift slightly exceeds the well-known bathochromic shift[56−61] observed in fluid solution upon changing from aqueous to less-polar solvents, such as dichloromethane. At higher loading levels (1:1 and 5:1), the intensities of the bands decrease, and the bands further shift to the red. Yam et al. have recently suggested that a decrease in the intensity of short-wavelength IL absorptions of platinum(II) diynyl complexes of terpyridine at high concentration is the result of the formation of aggregates.[62] (It should be noted that the Pt(5dπ) → π*(tpy) MLCT band is reasonably expected to maximize near 370 nm;[15,32,33,63] however, the transition is not well-resolved in any of the spectra.) The accumulated data suggest perturbation of the ligand energy levels in the rigid ZrP microenvironment, possibly as a result of intermolecular tpy···tpy interactions between complexes.[64]

To better assess the long-wavelength absorption properties of the platinum complex-exchanged ZrP samples, room-temperature diffuse reflectance spectra of the platinum salts and the intercalation materials at different loadings levels (Figures 7 and 8) were recorded. For both classes of intercalation compounds, there are additional long-wavelength absorption features that are not present in dilute fluid solutions of the platinum salts. In the case of $[Pt(Me_2bzimpy)Cl]^+$-exchanged ZrP powders, the reflectance spectra are qualitatively similar to that of $[Pt(Me_2bzimpy)Cl]Cl\cdot 2.5H_2O$. The platinum salt gives rise to a reflectance

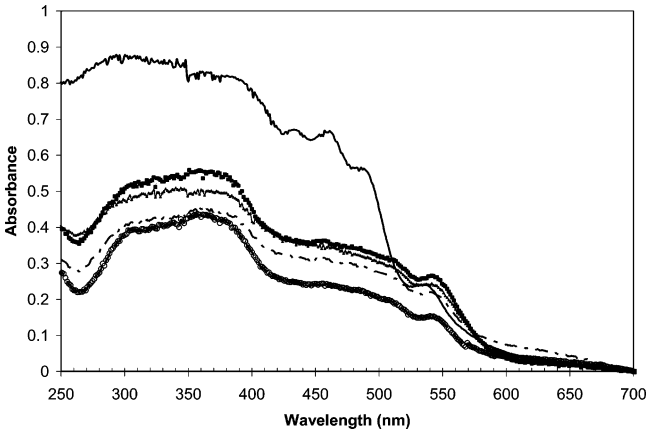

Figure 7. Room-temperature diffuse reflectance spectra of $[Pt(Me_2bzimpy)Cl]^+$-exchanged ZrP at different loadings (●, 1:30; ----, 1:10; ▲, 1:5; ■, 1:1) and $[Pt(Me_2bzimpy)Cl]Cl\cdot 2.5H_2O$ (—, solid line).

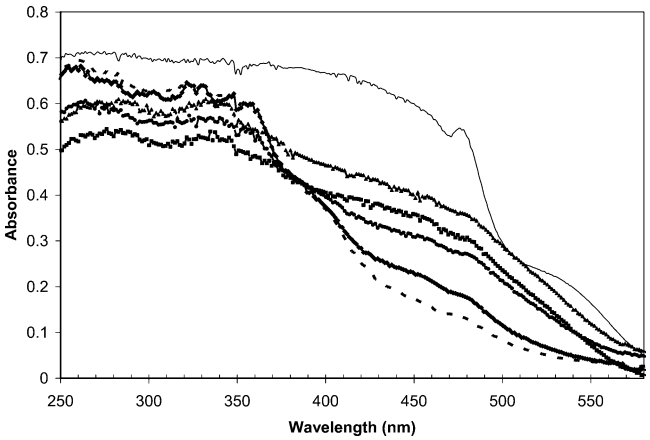

Figure 8. Room-temperature diffuse reflectance spectra of $[Pt(tpy)Cl]^+$-exchanged ZrP at different loadings (◆, 1:25; ----, 1:10; ●, 1:5; ■, 1:1; ▲, 5:1) and $[Pt(tpy)Cl]Cl\cdot 2H_2O$ (—, solid line).

(56) Michalec, J. F.; Bejune, S. A.; Cuttell, D. G.; Summerton, G. C.; Gertenbach, J. A.; Field, J. S.; Haines, R. J.; McMillin, D. R. *Inorg. Chem.* **2001**, *40*, 2193−2200.
(57) Cummings, S. D.; Eisenberg, R. *J. Am. Chem. Soc.* **1996**, *118*, 1949−1960.
(58) Pomestchenko, I. E.; Castellano, F. N. *J. Phys. Chem. A* **2004**, *108*, 3485−3492.
(59) Willison, S. A.; Jude, H.; Antonelli, R.; Rennekamp, J. M.; Eckert, N.; Krause, J.; Connick, W. B. *Inorg. Chem.* **2004**, *43*, 2548−2555.
(60) McGarrah, J. E.; Eisenberg, R. *Inorg. Chem.* **2003**, *42*, 4355−4365.
(61) Vanhelmont, F. W. M.; Johnson, R. C.; Hupp, J. *Inorg. Chem.* **2000**, *39*, 1814−1816.
(62) Yam, V. W. W.; Wong, K. M. C.; Zhu, N. *J. Am. Chem. Soc.* **2002**, *124*, 6506−6507.
(63) Aldridge, T.; Stacy, E.; McMillin, D. R. *Inorg. Chem.* **1994**, *33*, 722−727.
(64) Colón, J. L.; Yang, C.; Clearfield, A.; Martin, C. R. *J. Phys. Chem.* **1988**, *92*, 5777−5781.

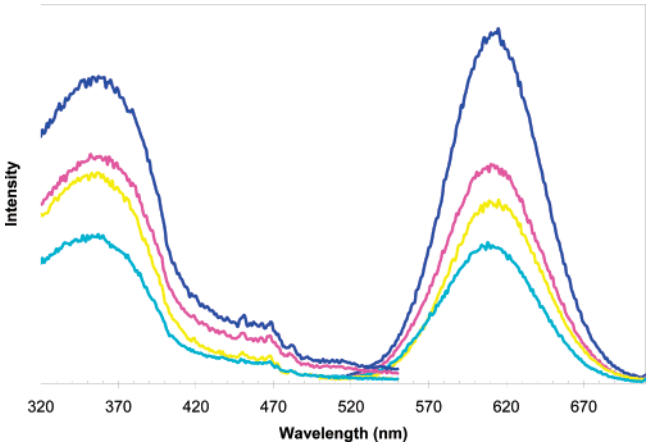

Figure 9. Room-temperature emission (λ_{ex} = 355 nm) and excitation (λ_{em} = 612 nm) spectra of [Pt(Me$_2$bzimpy)Cl]$^+$-exchanged ZrP methanol suspensions (0.008% w/v) at different loading levels: (blue, 1:1), (pink, 1:5), (yellow, 1:10), (cyan, 1:30).

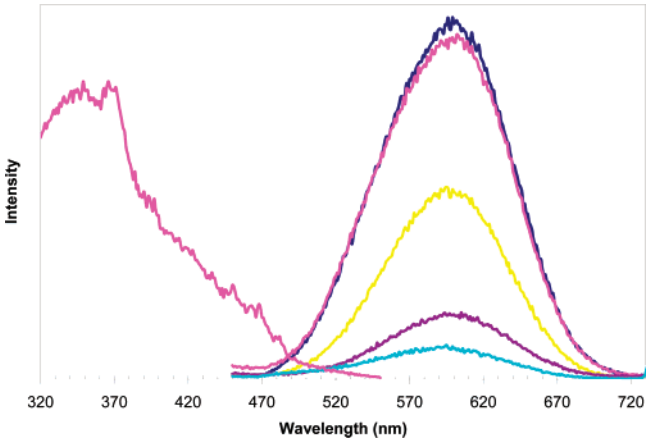

Figure 10. Room-temperature emission (λ_{ex} = 366 nm) and excitation (λ_{em} = 600 nm) spectra of [Pt(tpy)Cl]$^+$-exchanged ZrP aqueous suspensions (0.008% w/v) at different loading levels: (navy blue, 5:1), (pink, 1:1), (yellow, 1:5), (dark purple, 1:10), and (cyan, 1:25).

maximum at 536 nm. Although the structure of these materials is not known, by analogy to previous work,[38] the band is reasonably attributed to a spin-allowed MMLCT-[dσ*(Pt) → π*(tpy)] transition resulting from short Pt···Pt interactions. Upon intercalation, the band shifts by 170 cm^{-1} to 541 nm, suggesting slightly stronger intermolecular interactions.

In the case of [Pt(tpy)Cl]$^+$, the long wavelength absorption bands are poorly resolved, although a distinct shoulder occurs near 475 nm, co-incident with a maximum in the reflectance spectrum of [Pt(tpy)Cl]Cl·2H$_2$O. Bands at nearly the same wavelength in the spectra of related platinum(II) terpyridyl complexes have been assigned to a spin-allowed MMLCT transition;[31,32,65] however, the assignment in the present case is not certain. For example, the terpyridyl-centered $^3\pi-\pi^*$ transition of [Pt(tpy)Cl]$^+$ is known to maximize at 463 nm,[32] and we have already noted that the ^{1}IL transitions of the intercalated material are shifted significantly to the red. At longer wavelengths, the reflectance gradually tails off with no well-resolved features. By contrast, the reflectance spectrum of [Pt(tpy)Cl]Cl·2H$_2$O shows a broad shoulder near 540 nm. The [Pt(tpy)Cl]$^+$ cations pack in a head-to-tail fashion to form dimers in crystals of [Pt(tpy)Cl]Cl·2H$_2$O with relatively short (~3.4 Å) Pt···Pt distances,[51,66] suggesting that the 540 nm band of the chloride salt arises from a low-lying MMLCT transition.

At room temperature, the platinum complex-exchanged ZrP materials are brightly emissive as powders (Supporting Information Figures S4 and S5) or in colloidal suspensions (Figures 9 and 10). This result is somewhat surprising since neither [Pt(Me$_2$bzimpy)Cl]$^+$ nor [Pt(tpy)Cl]$^+$ is emissive in room-temperature fluid solution.[13,15,38,56,63] For both classes of intercalated materials, the emission intensity increases steadily with increasing loading. The emission profiles are unstructured and shifted to the red of the vibronically structured emissions observed for the free complexes in 77 K dilute glassy solutions ([Pt(Me$_2$bzimpy)Cl]$^+$, 545 and 590 nm);[31] [Pt(tpy)Cl]$^+$, 475, 507, and 544 nm).[22] The resulting excitation spectra are in agreement with the diffuse reflectance spectra, showing long-wavelength features that are absent from the absorption spectra of dilute fluid solutions of the platinum salts. Taken together, these observations point to the influence of intermolecular interactions on the lowest emissive states.

In the case of the [Pt(Me$_2$bzimpy)Cl]$^+$-exchanged ZrP, the room-temperature emissions from [Pt(Me$_2$bzimpy)Cl]$^+$-exchanged ZrP originate from a lowest MMLCT state. The emission profile is characteristically symmetric and narrow (full-width at half-maximum (fwhm), ~1950 cm^{-1}), maximizing at 612 nm. The spectra are slightly shifted to shorter wavelengths than those of room-temperature solid-state samples of methanol vapor-exposed [Pt(Me$_2$bzimpy)Cl](Cl) (643 nm, fwhm, 2100 cm^{-1}), suggesting somewhat longer Pt···Pt separations.[38] By contrast, the [Pt(tpy)Cl]$^+$-exchanged ZrP gives rise to a broad, asymmetric emission band maximizing near 600 nm with a fwhm of ~3040 cm^{-1}. As the loading level increases up to 1:10 Pt/ZrP, the emission maximum shifts by ~150 cm^{-1} to longer wavelengths; at higher levels, the maximum remains unchanged. The observed behavior is different than that of Pt(tpy)Cl$^+$ in 77 K frozen solution, where a unimolecular vibronically structured emission (λ_{max}, 475, 507, and 544 nm) dominates at low concentration and longer wavelength emissions ($\lambda_{max} \geq$ 600 nm) due to aggregates grown at higher concentrations. Interestingly, the asymmetry of the [Pt(tpy)Cl]$^+$-exchanged ZrP emission band manifests as a skewing of the emission maximum toward *longer* wavelengths, which is the opposite of what is encountered for unimolecular MLCT emissions of platinum(II) polypyridyl complexes.[31,34,56,67] Similarly, MMLCT emissions of aggregates tend to be symmetric or slightly asymmetric with maxima skewed toward shorter wavelengths because of poorly resolved vibronic structure.[19,23,66] While it is premature to make a definitive assignment, it is noteworthy that the observed emissions bear

(65) Kobayashi, K.; Sato, H.; Shinobu, K.; Kato, M.; Ishizaka, S.; Kitamura, N.; Yamagishi, A. *J. Phys. Chem. B.* **2004**, *108*, 18665−18669.
(66) Miskowski, V. M.; Houlding, V. H. *Inorg. Chem.* **1991**, *30*, 4446−4452.
(67) Connick, W. B.; Miskowski, V. M.; Houlding, V. H.; Gray, H. B. *Inorg. Chem.* **2000**, *39*, 2585−2592.

a resemblance to those of various orange and yellow [Pt(tpy)Cl]$^+$ salts (PF_6^-, 630 nm; Cl^-, 650 nm; ClO_4^-, 645 nm; $CF_3SO_3^-$, 640 nm; fwhm, 3000−4250 cm^{-1}) at room temperature. The emissions from those materials has been assigned to a lowest IL excimeric state arising from tpy···tpy interactions.[32]

Conclusion

[Pt(tpy)Cl]$^+$ and [Pt(Me$_2$bzimpy)Cl]$^+$ are readily ion-exchanged into 10.3 Å-ZrP to give novel luminescent materials. Spectroscopic measurements show that the physical and chemical structures of the complexes and the layers are maintained. The results are consistent with an expansion of the interlayer spacing to ∼18 Å to accommodate aggregates of closely interacting platinum complexes. [Pt(Me$_2$bzimpy)Cl]$^+$-exchanged ZrP exhibits distinct absorption and emission spectroscopic signatures that are independent of loading levels and characteristic of low-lying MMLCT states resulting from short Pt···Pt spacings. By contrast, the spectroscopic properties of [Pt(tpy)Cl]$^+$-exchanged ZrP are dependent on loading levels, suggesting the existence of more than one type of intercalated platinum aggregate. At high loading levels, [Pt(Me$_2$bzimpy)Cl]$^+$ and [Pt(tpy)Cl]$^+$ ions can serve as pillars inside the ZrP framework. Overall, these results open the door to a rich and relatively unexplored area that takes advantage of the tendency of the negatively charged ZrP scaffold to promote formation of rather well-defined, high-density assemblies of platinum(II) cations.

Acknowledgment. We wish to thank Dr. Antonio Martínez and the staff of UPR's Material Characterization Center for their help with the XRPD, FT-IR, and XPS measurements. We also thanks Dr. Angel Martí, Dr. Ricardo Bermúdez, Dr. Mitk'El Santiago, and Agustín Díaz for their helpful discussions and technical assistance.

Supporting Information Available: Figures S1−S5 in PDF format. This material is available free of charge via the Internet at http://pubs.acs.org.

IC7006183